A malaria membrane skeletal protein is essential for normal morphogenesis, motility, and infectivity of sporozoites

Emad I. Khater, Robert E. Sinden, and Johannes T. Dessens

Department of Biological Sciences, Imperial College London, London SW7 2AZ, England, UK

Membrane skeletons are structural elements that provide mechanical support to the plasma membrane and define cell shape. Here, we identify and characterize a putative protein component of the membrane skeleton of the malaria parasite. The protein, named PbIMC1a, is the structural orthologue of the *Toxoplasma gondii* inner membrane complex protein 1 (TgIMC1), a component of the membrane skeleton in tachyzoites. Using targeted gene disruption in the rodent malaria species *Plasmodium berghei*, we show that PbIMC1a is involved in sporozoite development, is necessary for providing normal sporozoite cell shape and mechanical stability, and is essential for sporozoite infectivity in insect and vertebrate hosts. Knockout of PbIMC1a protein expression reduces, but does not abolish, sporozoite gliding locomotion. We identify a family of proteins related to PbIMC1a in *Plasmodium* and other apicomplexan parasites. These results provide new functional insight in the role of membrane skeletons in apicomplexan parasite biology.

Introduction

Apicomplexan parasites cause major diseases in humans and animals. Amongst these is featured malaria, which remains the most important parasitic human disease responsible for millions of deaths per year. Malaria parasites have a complex life cycle involving many life stages as well as mosquito and vertebrate hosts. Sporozoites infect both hosts and play a vital role in malaria transmission. They possess a specialized cortical structure, the pellicle, which is composed of the plasma membrane and a tightly associated inner membrane complex (IMC). Underneath the IMC lie subpellicular microtubules (SMT), which extend for about two thirds of the cell starting from the apical end. The sporozoite pellicle and associated cytoskeletal elements are conserved in the other invasive stages of *Plasmodium*, ookinetes and merozoites, as well as in invasive stages of other apicomplexan parasites (for review see Morrissette and Sibley, 2002).

Recently, the subpellicular network (SPN) was identified in *Toxoplasma gondii* tachyzoites (Mann and Beckers, 2001). The SPN is a two-dimensional network of filaments situated on the cytoplasmic side of the IMC that takes the shape of the cell and is resilient to detergent extraction, indicating that it acts as a membrane skeleton (Mann and Beckers, 2001). Two structurally unrelated proteins of the tachyzoite SPN, named TgIMC1 and TgIMC2, were identified. TgIMC1 shares sequence homology with articulins, proteins of membrane skeletons of free-living protists, and has been implicated in SPN maturation during development of daughter parasites (Mann and Beckers, 2001; Hu et al., 2002; Mann et al., 2002). The existence of a similar filamentous network in other apicomplexan parasites has been described previously (D'Haese et al., 1977). Moreover, a homologue of TgIMC1 exists in the human malaria species *Plasmodium falciparum* (Mann and Beckers, 2001), indicating that the SPN is not confined to *T. gondii* tachyzoites, but constitutes a conserved structure across the Apicomplexa.

Despite the central role of membrane skeletons in cell development, shape, and structural integrity, little is known of the molecular composition and function of the membrane skeleton in malaria parasites. In this paper we identify and characterize the structural orthologue of the membrane skeletal protein TgIMC1 in the rodent malaria parasite *Plasmodium berghei* and shed light on its role in the parasite life cycle.

The online version of this article includes supplemental material.

Correspondence to J.T. Dessens: j.dessens@imperial.ac.uk

Abbreviations used in this paper: IFA, immunofluorescent antibody; IMC, inner membrane complex; SMT, subpellicular microtubules; SPN, subpellicular network; WT, wild-type.

Results and discussion

Identification of a TgIMC1 orthologue in *P. berghei*

We used BLAST homology searches with the TgIMC1 amino acid sequence to identify orthologous genes in *Plasmodium*. The

The Journal of Cell Biology, Vol. 167, No. 3, November 8, 2004 425–432
http://www.jcb.org/cgi/doi/10.1083/jcb.200406068

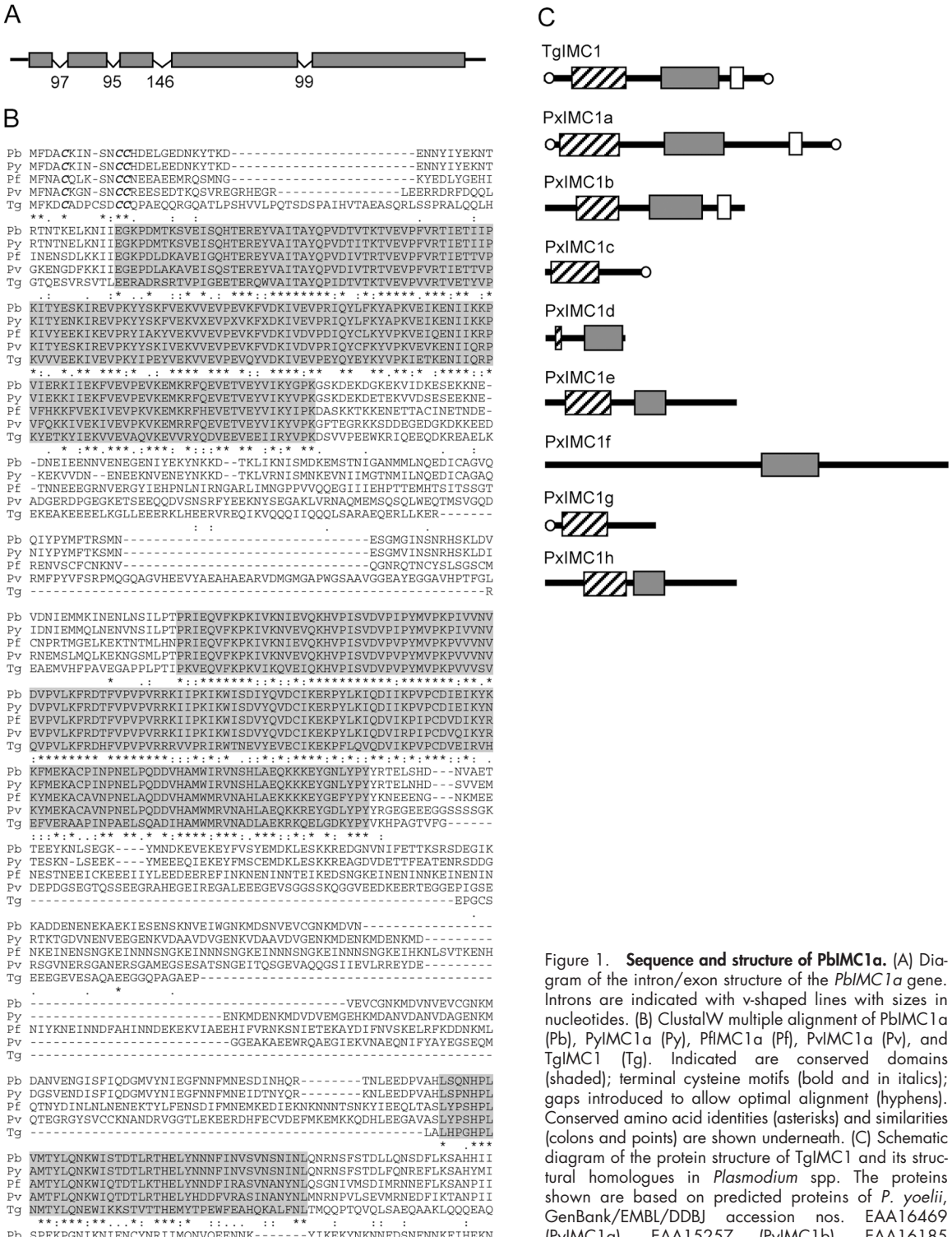

Figure 1. **Sequence and structure of PbIMC1a.** (A) Diagram of the intron/exon structure of the *PbIMC1a* gene. Introns are indicated with v-shaped lines with sizes in nucleotides. (B) ClustalW multiple alignment of PbIMC1a (Pb), PyIMC1a (Py), PfIMC1a (Pf), PvIMC1a (Pv), and TgIMC1 (Tg). Indicated are conserved domains (shaded); terminal cysteine motifs (bold and in italics); gaps introduced to allow optimal alignment (hyphens). Conserved amino acid identities (asterisks) and similarities (colons and points) are shown underneath. (C) Schematic diagram of the protein structure of TgIMC1 and its structural homologues in *Plasmodium* spp. The proteins shown are based on predicted proteins of *P. yoelii*, GenBank/EMBL/DDBJ accession nos. EAA16469 (PyIMC1a), EAA15257 (PyIMC1b), EAA16185 (PyIMC1c), EAA17029 (PyIMC1d), EAA15249 (PyIMC1e), EAA15609 (PyIMC1f), EAA15402 (PyIMC1g), and EAA20426 (PyIMC1h). Boxes mark domains corresponding to the conserved amino-terminal domain (hatched), central domain (gray), and carboxy-terminal domain (open). Conserved terminal cysteine motifs are indicated with open circles.

highest sequence homology (33% amino acid identity) was found with a predicted protein of *Plasmodium yoelii*. We designed primers to this gene to PCR amplify the cognate gene in *P. berghei*. Sequence analysis of two distinct PCR products amplified from genomic and cDNA, respectively, allowed us to map four introns in the *P. berghei* gene, named *PbIMC1a* (Fig. 1 A). The sequence data have been submitted to the GenBank database under accession no. AF542052. The orthologous genes in *P. yoelii* (*PyIMC1a*), *P. falciparum* (*PfIMC1a*) and *Plasmodium vivax* (*PvIMC1a*) are also predicted to contain four introns each at similar positions to those found experimentally in *PbIMC1a*.

The *PbIMC1a* mRNA encodes a predicted cytoplasmic protein of 784 amino acids with a calculated mass of 91,699. Amino acid alignment of PbIMC1a with its orthologues reveals three domains of high sequence conservation (Fig. 1 B). These three domains are separated by regions of variable amino acid composition and length. The amino-terminal and central conserved domains, albeit distinct, are both rich in valine (V) and proline (P) and have homology to the VP-rich core domain of articulins from free-living protists. The proteins are further characterized by conserved cysteine motifs at both the amino- and carboxy-terminal ends (Fig. 1 B). PbIMC1a and PyIMC1a share 80% amino acid identity, reflecting the close ancestry of these two rodent malaria parasite species. Lower, 44–45% identity is found between orthologues of the rodent and human malaria species, whereas the two human malaria species share 51% identity in this protein.

We identified another seven conserved *Plasmodium* proteins with significant sequence homology to PxIMC1a (PxIMC1b to h) containing up to three of the conserved domains (Fig. 1 C). Various homologues can also be identified in the genome sequences available from *Cryptosporidium*, *Toxoplasma*, *Babesia*, and *Eimeria* species (unpublished data), suggesting these molecules belong to a new gene family confined to the Apicomplexa.

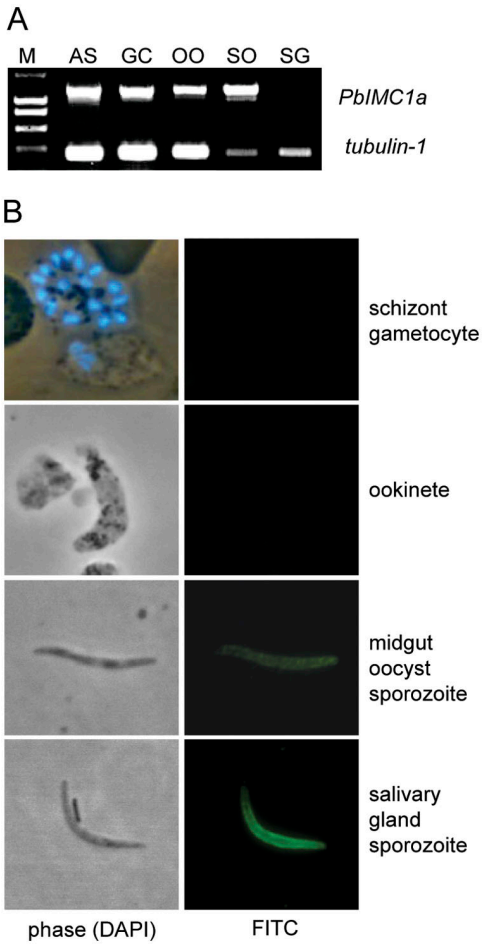

Figure 2. **Transcription and expression of PbIMC1a.** (A) RT-PCR analysis of *PbIMC1a* and *tubulin-1* mRNA in samples of asexual blood stages (AS), gametocytes (GC), ookinetes (OO), midguts with sporulating oocysts (SO), and sporozoite-infected salivary glands (SG). M: molecular weight markers. (B) IFA staining (FITC) of different life stages with anti-PbIMC1a antiserum. Phase: phase contrast. Blood stages are double-stained with DAPI (blue) to show merozoite and gametocyte nuclei.

Expression and localization of PbIMC1a

We studied transcription of the *PbIMC1a* gene by RT-PCR analysis in different life stages of the parasite using cDNA-specific primers. *PbIMC1a*-specific mRNA was detected in samples of asexual blood stages, gametocytes, ookinetes, and sporulating oocysts. The highest amount of *PbIMC1a*-specific mRNA with respect to the reference gene *tubulin-1* was present in sporulating oocysts, whereas *PbIMC1a* transcription was down-regulated in samples of sporozoite-infected mosquito salivary glands (Fig. 2 A).

To investigate PbIMC1a protein expression we raised polyclonal antisera to a region of the protein predicted to have high antigenicity and unique epitopes. Immunofluorescent antibody (IFA) staining with the anti-PbIMC1a immune serum labeled sporozoites, but failed to label asexual and sexual life stages including mature schizonts (containing merozoites), gametocytes, and ookinetes (Fig. 2 B). These results indicate that PbIMC1a is predominantly expressed during sporogony. Sporozoites isolated from sporulating oocysts and from salivary glands stained positive for PbIMC1a (Fig. 2 B). Salivary gland sporozoites typically showed peripheral staining. Moreover, these sporozoites failed to label in live staining (unpublished data). This localization pattern is thus consistent with the position of the IMC/SPN.

The sporozoite-specific expression of PbIMC1a suggests the parasite uses different proteins to fulfil functionally equivalent roles in the other invasive stages. The homologues of PbIMC1a are prime candidates. Indeed, we detected *PbIMC1b* mRNA in ookinete samples only (unpublished data), suggesting that PbIMC1b could carry out the equivalent role of PbIMC1a in this life stage. Mature schizonts of *P. falciparum* were reported to express a protein recognized by anti-TgIMC1 immune serum, indicating that a homologue of TgIMC1 is also expressed in the merozoite stage (Mann and Beckers, 2001).

PbIMC1a gene disruption

To study the role of PbIMC1a we generated *PbIMC1a* gene-disrupted parasites. A modified *T. gondii* dihydrofolate reductase/thymidylate synthase (*DHFR/TS*) gene cassette (conferring resistance to pyrimethamine) was inserted into the

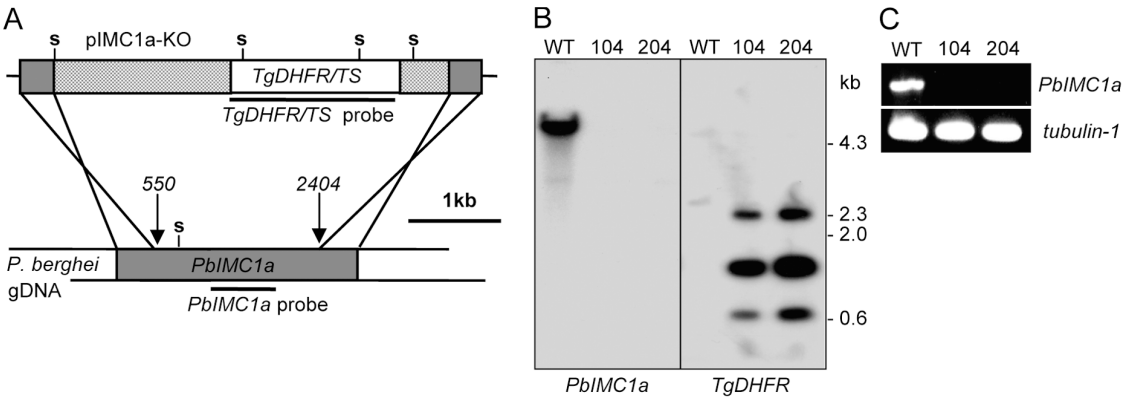

Figure 3. **Targeted disruption of *PbIMC1a*.** (A) Diagram of the recombination strategy. Indicated are sequences specific for *PbIMC1a* (dark gray); *PbDHFR* (light gray); *TgDHFR/TS* (white); positions of *Sph*I restriction sites (s); and probes used in Southern blot. (B) Southern analysis of SphI-digested genomic DNA (gDNA) from WT and PbIMC1a-KO parasite clones 104 and 204. (C) RT-PCR analysis of blood stages total RNA for mRNA of *PbIMC1a* and the reference gene *tubulin-1*.

PbIMC1a gene by double homologous recombination replacing nucleotides 550–2,404 of the *PbIMC1a* gene (Fig. 3 A). Southern analyses of SphI-digested genomic DNA from the resulting parasite (named PbIMC1a-KO) confirmed correct integration into the target locus: A probe corresponding to the central *PbIMC1a* region gave rise to a single band in parental wild-type (WT), but no signal in PbIMC1a-KO parasites. Conversely, a probe corresponding to the *DHFR/TS* gene gave rise to three *DHFR/TS*-specific bands in PbIMC1a-KO, but no signal in WT parasites (Fig. 3 B). In addition, *PbIMC1a*-specific mRNA was readily amplified by RT-PCR from total RNA samples of WT, but not from PbIMC1a-KO blood stage parasites, confirming disruption of the *PbIMC1a* gene (Fig. 3 C).

PbIMC1a-KO parasites developed normally in mice and were morphologically indistinguishable from WT parasites in Giemsa-stained blood films. Normal exflagellation and differentiation of gametocytes into ookinetes both in vitro and in vivo was observed (unpublished data). WT and PbIMC1a-KO parasite-infected *Anopheles stephensi* mosquitoes developed comparable numbers of oocysts in controlled experiments (Table I), indicating that the PbIMC1a-KO ookinetes are capable of normal midgut invasion and subsequent ookinete to oocyst transition. Oocysts in PbIMC1a-KO parasite-infected mosquitoes appeared to develop normally and formed large numbers of sporozoites (Table I). However, closer examination of these sporozoites revealed that they were of abnormal shape and some 20–30% smaller in size (Fig. 4, A and B). Each sporozoite possessed a single enlarged, protruding area associated with the position of the nucleus. The position of these protrusions varied between sporozoites from being located at the posterior end to being positioned near the middle of the sporozoite. Viability of oocyst and hemolymph sporozoites was comparable between WT and PbIMC1a-KO parasites (97–99%; $n = 100$), indicating that the abnormal cell shape was not the result of premature cell degeneration or death. This is supported by the fact that we did not observe sporozoites with normal morphology.

Western blot analysis of WT oocyst sporozoites gave rise to a major band of ~90 kD (Fig. 4 C), which likely corresponds to the full-length protein. No signal was detected in PbIMC1a-KO oocyst sporozoites (to compensate for the smaller size we loaded at least 50% more of the PbIMC1a-KO sporozoites). PbIMC1a-KO sporozoites were also negative in IFA staining (Fig. 4 D), demonstrating the specificity of the immune serum for PbIMC1a.

Ultrastructural examination of sporulating oocysts showed PbIMC1a-KO sporozoites being less homogeneous in shape

Table I. **Effects of PbIMC1a knockout on *P. berghei* parasite development in *A. stephensi* mosquitoes**

Experiment	Parasite [clone]	Mean ± SEM no. of oocysts per mosquito[a]	Percent infection	Mean no. of sporozoites per mosquito[b]		
				Midgut	Hemolymph	Salivary glands
I	WT	268 ± 34 (30)	100	10,190 (10)	N/A	6,880 (10)
	PbIMC1a-KO [104]	225 ± 30 (29)	100	12,420 (10)	N/A	0 (10)
	PbIMC1a-KO [204]	270 ± 33 (30)	100	24,000 (10)	N/A	0 (10)
II	WT	380 ± 53 (10)	100	26,630 (10)	N/A	1,940 (10)
	PbIMC1a-KO [104]	302 ± 69 (10)	100	14,000 (10)	N/A	0 (10)
III	WT	118 ± 19 (20)	100	31,000 (20)	4,800 (20)	69,660 (20)
	PbIMC1a-KO [104]	127 ± 18 (20)	100	36,330 (20)	1,530 (20)	0 (19)

Number of mosquitoes per sample indicated in parentheses. N/A, not assessed.
[a]Assessed at 9–11 d after infection.
[b]Assessed at 22–24 d after infection.

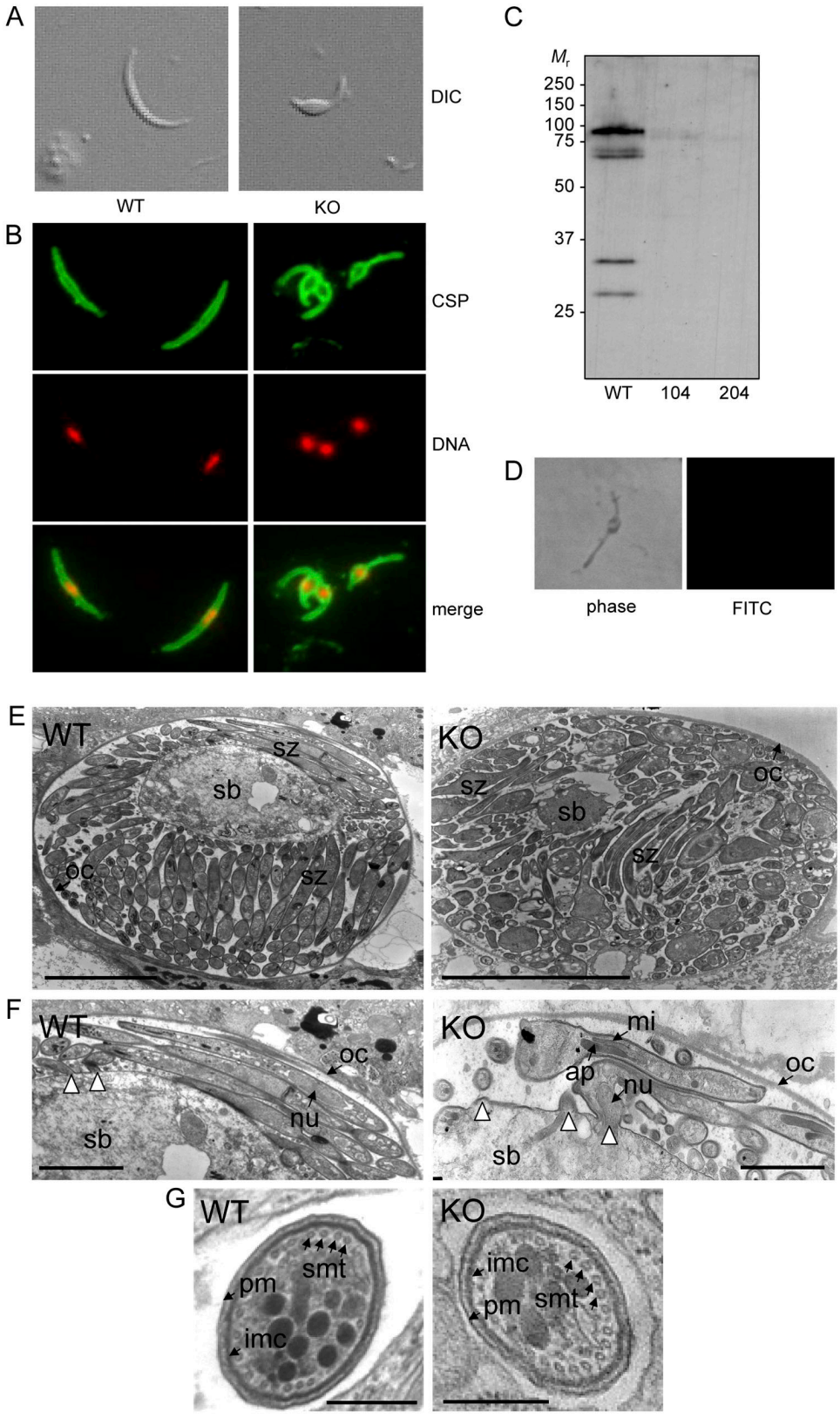

Figure 4. **Characteristics of PbIMC1a-KO sporozoites.** (A) Sporozoite shapes as observed by differential interference contrast (DIC). (B) Sporozoite shapes as observed by IFA staining for circumsporozoite protein (CSP, green) and DNA (red). (C) Western blot of oocyst sporozoites from WT and PbIMC1a-KO parasite clones 104 and 204. (D) Negative labeling of a PbIMC1a-KO sporozoite by IFA staining for PbIMC1a. (E) Cross section of sporulating oocysts. (F) Close-up view of E showing budding sporozoites. White arrowheads point at sporozoite budding sites. (G) Cross section of sporozoites. WT: wild-type, KO: PbIMC1a-KO, sb: sporoblast, sz: sporozoite, oc: oocyst wall, nu: nucleus, ap: apicoplast, mi: mitochondrion, pm: plasma membrane, imc: inner membrane complex, smt: subpellicular microtubules. Bars: 5 μm (E), 1 μm (F), 0.1 μm (G).

and size than their WT counterparts and, possibly as a consequence, arranged in a more disorganized fashion inside the oocyst (Fig. 4 E). Developing sporozoites in the process of budding from the sporoblast already appeared to possess the enlarged area around the nucleus (Fig. 4 F), indicating that the effect of the PbIMC1a knockout on cell shape occurs during or before this event. Apart from these visible abnormalities, PbIMC1a-KO sporozoites appeared to possess a complete set of organelles and the assembly of SMT and IMC appeared unaffected by the gene disruption (Fig. 4, F and G).

Given the similarities between *Plasmodium* sporozoite development by schizogony and *Toxoplasma* tachyzoite development by endodyogeny, both of which coincide with the assembly of IMC and SMT (Hu et al., 2002; Morrissette and Sibley, 2002), a role for PbIMC1a in sporozoite development is conceivable. In tachyzoites, and probably also in sporozoites, this process is concomitant with SPN formation (Mann et al., 2002). In nascent tachyzoites the SPN becomes more stable and rigid upon maturation, a process that is accompanied by proteolytic processing of TgIMC1 for which a conserved carboxy-terminal cysteine is required (Mann et al., 2002). A degree of proteolytic processing of PbIMC1a is also notable in oocyst sporozoites (Fig. 4 C), suggesting that formation of the SPN in sporozoites could involve a similar maturation step.

Infectivity and gliding motility of PbIMC1a-KO sporozoites

We were unable to detect PbIMC1a-KO sporozoites within or associated with the salivary glands (Table I). By contrast, substantial numbers of sporozoites were found in the hemolymph collected from PbIMC1a-KO parasite-infected mosquitoes (Table I). Arguably, these numbers were high enough to allow for detectable salivary gland invasion if the PbIMC1a-KO sporozoites were capable of normal motility, attachment, and invasion. We were also unable to infect naïve mice by injecting oocyst sporozoites of PbIMC1a-KO parasites under conditions where oocyst sporozoites of WT parasites were infective [4 infected mice out of 5 injected with WT sporozoites; 0 infected mice out of 5 injected with PbIMC1a-KO sporozoites]. These combined observations point to an inability of the mutant sporozoites to invade cells.

Gliding locomotion is necessary for cell invasion in sporozoites (Sultan et al., 1997). Therefore, we examined the ability of the sporozoites to glide in vitro. Observing live gliding of oocyst sporozoites on glass slides clearly showed that locomotion was compromised by the PbIMC1a knockout: null mutant sporozoites were able to attach normally to the glass surface and undergo circular gliding, but their gliding speed was fivefold slower than that of WT sporozoites (WT 2.5 ± 0.4 circles min^{-1}; PbIMC1a-KO 0.5 ± 0.1 circles min^{-1}; $n = 7$) (Fig. 5 A). Possibly as a consequence of the reduced speed, the percentage of attached PbIMC1a-KO sporozoites observed to be gliding within a set time frame was just half that of WT sporozoites (WT 32%; PbIMC1a-KO 17%; $n = 53$). These results indicate that PbIMC1a is not a vital component of the motility machinery of the cell, which is closely associated with the pellicle structure (for review see Kappe et al., 2004). Possibly,

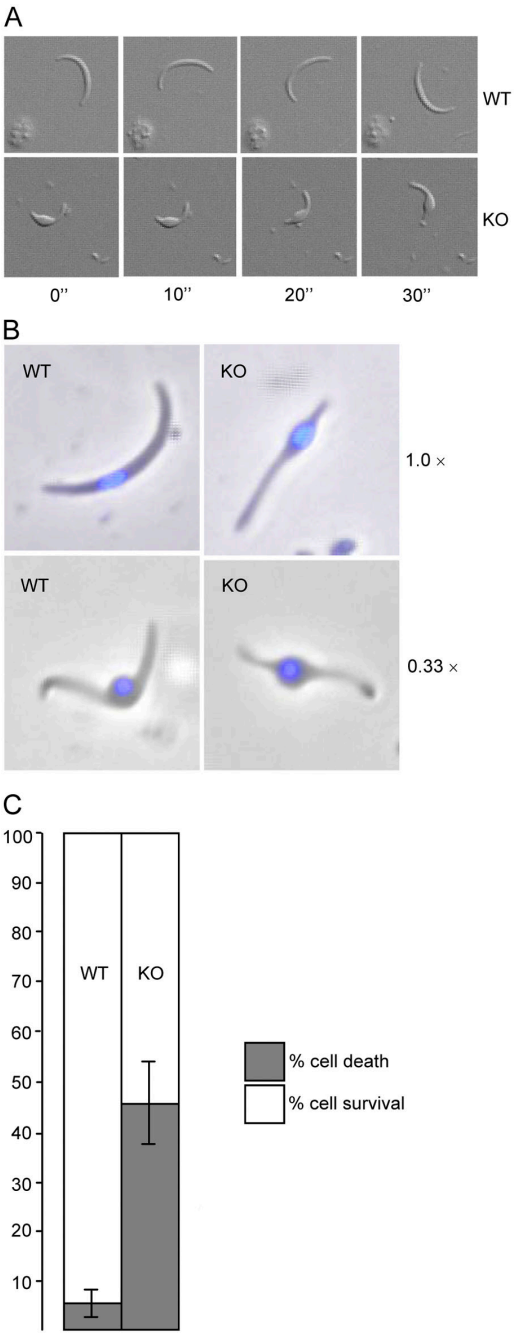

Figure 5. **Sporozoite gliding motility and resistance to osmotic shock.** (A) Circular gliding of sporozoites on glass slides. Frames are taken at 10-s intervals. (B) Swelling of sporozoites exposed to 0.33× normal osmotic strength, compared with untreated cells (1.0×). Nuclei are stained with DAPI (blue). (C) Percent sporozoite survival/death after hypo-osmotic shock (5-min exposure to 0.33× normal osmotic strength, values normalized to 100% viability in untreated cells). Error bars indicate SDs from two independent experiments. At least 100 cells were scored for each sample. WT: wild-type, KO: PbIMC1a-KO.

the reduced motility of the knockout sporozoites is an effect of their abnormal cell shape or size. Alternately, PbIMC1a may interact directly or indirectly with components of the gliding machinery. The molecular interactions involved in gliding are known to be complex and involve multiple protein components besides actin and myosin, such as myosin A tail domain-inter-

acting protein (Bergman et al., 2002), aldolase (Buscaglia et al., 2003; Jewett and Sibley, 2003), and membrane receptors (Gaskins et al., 2004). Given the opportunities for multiple protein interactions, as well as the existence of multiple PbIMC1a homologues, some functional redundancy may exist, resulting in reduced rather than abolished motility. Given the essential connection between gliding motility and cell invasion, the reduced motility of PbIMC1a-KO sporozoites could be partly or solely responsible for their lack of infectivity.

Mechanical stability of PbIMC1a-KO sporozoites

Assessment of the SPN as done for tachyzoites is difficult to do with sporozoites due to their small size and the lack of a culture system to produce large numbers of cells. These problems preclude a straightforward assessment of the presence and integrity of a SPN in WT and PbIMC1a-KO sporozoites. Given data from *T. gondii* studies and the known functions of membrane skeletons in general (Pumplin and Bloch, 1993), sporozoites with a disrupted SPN are likely to be compromised in their ability to withstand mechanical pressures from inside and outside the cell. This scenario conforms to the observed loss of function phenotypes. First, PbIMC1a-KO sporozoites are of abnormal shape and most notably possess a protruding area around the nucleus. The shape of the nucleus in these sporozoites is rounded, whereas in WT sporozoites the shape of the nucleus is elongated (Fig. 4 B), indicating that they are unable to confine the nucleus and its associated structures within the normally narrow sporozoite frame. Second, PbIMC1a-KO sporozoites appear incapable of cell invasion. Considerable mechanical pressures are applied to sporozoites when they invade cells. Hence, a weakened membrane skeleton could prevent PbIMC1a-KO sporozoites from successfully completing the process of cell invasion.

To assess whether PbIMC1a knockout had affected the mechanical stability of the parasite, we subjected sporozoites to hypo-osmotic shock. Hypo-osmotic conditions cause cells to draw in water and swell, and the degree of hypo-osmotic stress a cell can tolerate is a measure of its mechanical strength (Menke and Jockusch, 1991). Under hypo-osmotic conditions both WT and PbIMC1a-KO sporozoites swelled in one particular area of the cell, namely around the nucleus (Fig. 5 B). Exposure of the cells to 5 min of hypo-osmotic stress caused only a small degree (6.5%) of cell death in WT sporozoites. By contrast, the same treatment caused more than sevenfold higher (47%) cell death in PbIMC1a-KO sporozoites practically halving the population of viable sporozoites (Fig. 5 C). These results show that PbIMC1a-KO sporozoites have considerably lower resistance to osmotic shock, indicating that their ability to withstand mechanical pressure is adversely affected by the *PbIMC1a* gene disruption. This is consistent with PbIMC1a being a membrane skeleton component.

Materials and methods

Parasite maintenance, culture, and purification; mosquito infections; and Southern and Western blotting were performed as described previously (Dessens et al., 1999; Sinden et al., 2002). Sporozoite gliding was assessed as described previously (Vanderberg, 1974; Sultan et al., 1997).

Sporozoite preparation, viability, and osmotic shock

Oocyst, hemolymph, and salivary gland sporozoites were isolated as described previously (Kariu et al., 2002) For viability assessment, sporozoites were incubated for 10 min in medium supplemented with 5 mg/l propidium iodide and 1% Hoechst 33258, and were examined by fluorescence microscopy. Sporozoites whose nucleus stained positive for both propidium iodide and Hoechst were scored as nonviable, those staining positive only for Hoechst were scored as viable. Sporozoites were subjected to hypo-osmotic shock (0.33× normal osmotic strength) by adding two equal volumes of water. After 5 min the osmotic strength of the media was returned to normal by adding an appropriate amount of 10× PBS and cell viability was scored.

Cloning of *PbIMC1a*

Parasite genomic DNA and cDNA was prepared as described previously (Dessens et al., 1999). For cloning of *PbIMC1a*, primers P1F and P1R, designed to the predicted 5′ and 3′ coding sequence of *PyIMC1a*, were used in PCR amplification on *P. berghei* cDNA and genomic DNA. PCR products were analyzed by automated sequencing and primer walking. Stage-specific transcription of *PbIMC1a* was determined by RT-PCR using cDNA-specific primers P7F and P7R on different life stages as described previously (Claudianos et al., 2002).

Construction of transgenic parasites

A 5′ portion of *PbIMC1a* was amplified with primers P13F-KpnI and P13R-HindIII, digested with KpnI and HindIII, and ligated into KpnI/HindIII-digested pBS-DHFR (Dessens et al., 1999) to give pIMC1-KH. A 3′ portion of *PbIMC1a* was amplified with primers P14F-XbaI and P14R-NotI, digested with XbaI and NotI, and ligated into XbaI/NotI-digested pIMC1-KH to give the transfection plasmid pIMC1a-KO. 50 μg KpnI/NotI-digested pIMC1-KO was transfected into purified schizonts followed by pyrimethamine selection and limiting dilution cloning as described previously (Waters et al., 1997).

Antibody production

The *PbIMC1a* coding sequence corresponding to residues 456–632 was PCR amplified with primers P22F-BamHI and P23R-XhoI, digested with BamHI and XhoI, and ligated into BamHI/XhoI-digested pGEX-4T-1 (Amersham Biosciences) to give pGEX-rPbIMC1a4. Expression and purification of the resulting GST/PbIMC1a fusion protein and antiserum production in mice was as described previously (Dessens et al., 2003).

Immunofluorescence and electron microscopy

Parasites were spotted on multiwell microscope slides, air dried, and heated on a hot plate at 98°C for 1 min. IFA staining was performed as described previously (Claudianos et al., 2002) using anti-PbIMC1a immune serum as primary antibody diluted 1:100, and goat anti–mouse FITC-conjugated secondary antibody (Sigma-Aldrich) diluted 1:100. Samples were mounted in Vectashield with DAPI (Vector Laboratories) and examined at RT on a DMR microscope (Leica) with a 100×/1.35 oil immersion objective lens. Images were acquired using a camera (DC500; Leica) and IM1000 image manager software (Leica). Mosquito midguts with sporulating oocysts were prepared for transmission electron microscopy as described previously (Sinden et al., 1985) and were examined with a transmission electron microscope (EM 400T; Philips).

Online supplemental material

Table S1 shows sequences of oligonucleotide primers. Online supplemental material available at http://www.jcb.org/cgi/content/full/jcb.200406068/DC1.

We thank Charles Claudianos for helpful discussions.

E.I. Khater was supported by an Islamic Development Bank Merit Scholarship Program in High Technology. J.T. Dessens was supported by the Wellcome Trust.

Submitted: 11 June 2004
Accepted: 15 September 2004

References

Bergman, L.W., K. Kaiser, H. Fujioka, I. Coppens, T.M. Daly, S. Fox, K. Matuschewski, V. Nussenzweig, and S.H. Kappe. 2002. Myosin A tail domain interacting protein (MTIP) localizes to the inner membrane complex of *Plasmodium* sporozoites. *J. Cell Sci.* 116:39–49.

Buscaglia, C.A., I. Coppens, W.G. Hol, and V. Nussenzweig. 2003. Sites of interaction between aldolase and thrombospondin-related anonymous protein in *Plasmodium. Mol. Biol. Cell.* 14:4947–4957.

Claudianos, C., J.T. Dessens, H.E. Trueman, M. Arai, J. Mendoza, G. Butcher, T. Crompton, and R.E. Sinden. 2002. A malaria scavenger receptor-like protein essential for parasite development. *Mol. Microbiol.* 45:1473–1484.

Dessens, J.T., A.L. Beetsma, G. Dimopoulos, K. Wengelnik, A. Crisanti, F.C. Kafatos, and R.E. Sinden. 1999. CTRP is essential for mosquito infection by malaria ookinetes. *EMBO J.* 18:6221–6227.

Dessens, J.T., I. Sidèn-Kiamos, J. Mendoza, V. Mahairaki, E. Khater, D. Vlachou, X. Xu, F.C. Kafatos, C. Louis, G. Dimopoulos, and R.E. Sinden. 2003. SOAP, a novel malaria ookinete protein involved in mosquito midgut invasion and oocyst development. *Mol. Microbiol.* 49:319–329.

D'Haese, J., H. Melhorn, and W. Peters. 1977. Comparative electron microscope study of pellicular structures in coccidia (*Sarcosystis*, *Besnoitia* and *Eimeria*). *Int. J. Parasitol.* 7:505–518.

Gaskins, E., S. Gilk, N. DeVore, T. Mann, G. Ward, and C. Beckers. 2004. Identification of the membrane receptor of a class XIV myosin in *Toxoplasma gondii. J. Cell Biol.* 165:383–393.

Hu, K., T. Mann, B. Striepen, C. Beckers, D.S. Roos, and J.M. Murray. 2002. Daughter cell assembly in the protozoan parasite *Toxoplasma gondii. Mol. Biol. Cell.* 13:593–606.

Jewett, T.J., and L.D. Sibley. 2003. Aldolase forms a bridge between cell surface adhesins and the actin cytoskeleton in apicomplexan parasites. *Mol. Cell.* 11:885–894.

Kappe, S.H.I., C.A. Buscaglia, L.W. Bergman, I. Coppens, and V. Nussenzweig. 2004. Apicomplexan gliding motility and host cell invasion: overhauling the motor model. *Trends Parasitol.* 20:13–16.

Kariu, T., M. Yuda, K. Yano, and Y. Chinzei. 2002. MAEBL is essential for malarial sporozoite infection of the mosquito salivary gland. *J. Exp. Med.* 195:1317–1323.

Mann, T., and C. Beckers. 2001. Characterization of the subpellicular network, a filamentous membrane skeletal component in the parasite *Toxoplasma gondii. Mol. Biochem. Parasitol.* 115:257–268.

Mann, T., E. Gaskins, and C. Beckers. 2002. Proteolytic processing of TgIMC1 during maturation of the membrane skeleton of *Toxoplasma gondii. J. Biol. Chem.* 277:41240–41246.

Menke, A., and H. Jockusch. 1991. Decreased osmotic stability of dystrophinless muscle cells from the mdx mouse. *Nature.* 349:69–71.

Morrissette, N.S., and L.D. Sibley. 2002. Cytoskeleton of apicomplexan parasites. *Microbiol. Mol. Biol. Rev.* 66:21–38.

Pumplin, D.W., and R.J. Bloch. 1993. The membrane skeleton. *Trends Cell Biol.* 3:113–117.

Sinden, R.E., R.H. Hartley, and L. Winger. 1985. The development of *Plasmodium* ookinetes in vitro: an ultrastructural study including a description of meiotic division. *Parasitology.* 91:227–244.

Sinden, R.E., G.A. Butcher, and A.L. Beetsma. 2002. Maintenance of the *Plasmodium berghei* life cycle. *Methods Mol. Med.* 72:25–40.

Sultan, A.A., V. Thathy, U. Frevert, K.J. Robson, A. Crisanti, V. Nussenzweig, R.S. Nussenzweig, and R. Ménard. 1997. TRAP is necessary for gliding motility and infectivity of *Plasmodium* sporozoites. *Cell.* 90:511–522.

Vanderberg, J.P. 1974. Studies on the motility of *Plasmodium* sporozoites. *J. Protozool.* 21:527–537.

Waters, A.P., A.W. Thomas, M.R. van Dijk, and C.J. Janse. 1997. Transfection of malaria parasites. *Methods.* 13:134–147.